DOI 10.1007/s11106-023-00382-5
Powder Metallurgy and Metal Ceramics, Vol. 62, Nos. 3-4, July, 2023 (Ukrainian Original Vol. 62, Nos. 3-4, March-April, 2023)

REFRACTORY AND CERAMIC MATERIALS

ELECTROCALORIC EFFECT OF Sm-DOPED 0.5BZT–0.5BCT LEAD-FREE CERAMICS

Fengji Zheng,[1] Shijuan Lu,[1] Xue Tian,[1] Xiaodong Jiang,[1] Ze Fang,[1] and Yongcheng Zhang[1,2]

UDC 621.565.8:53.082.74:666.654

The use of refrigeration technology is widespread in national security, industrial and agricultural production, biomedicine, and everyday life. High efficiency, environmental friendliness, and low cost make solid-state refrigeration based on electrocaloric effect (ECE) a promising refrigeration technology. Lead-free ferroelectric ceramics $(1–x)Ba(Zr_{0.2}Ti_{0.8})O_3–x(Ba_{0.7}Ca_{0.3})TiO_3$ (BZT–BCT) are promising materials for electrocaloric refrigeration in the field. In this paper, Sm-doped 0.5BZT–0.5BCT ceramic was fabricated by the conventional solid-state reaction method. The effect of Sm-doping contents (0, 1.0, 2.0, 2.5, and 3.0 mol.%) on the phase structures, dielectric properties, ferroelectricity, and electrocaloric properties of 0.5BZT–0.5BCT ceramics was systematically examined. The results indicate that all ceramics have a pure perovskite structure with no other secondary phase available. High relative densities are observed in all lead-free ferroelectric ceramics and all of the samples show transgranular fracture with no clear grain boundaries seen. The ceramics' ferroelectric hysteresis loops become thinner as the Sm doping content increases. At that, remanent polarization Pr decreases, indicating that more polar nanoregions (PNRs) are formed in BZT–BCT lead-free ceramics through Sm doping. The increase in Sm doping content resulted in a change in the dielectric permittivity and electrocaloric temperature that first increased and then decreased. The maximum dielectric permittivity is 5,518 when the doping content of Sm is 2.5 mol.% and the maximum electrocaloric temperature change ΔT_{max} of 0.109 K at 4 kV/mm was obtained when Sm doping content was 2 mol.%. The results show that an appropriate Sm doping is favorable for improving the dielectric, ferroelectric, and electrothermal properties of lead-free ceramics 0.5BZT–0.5BCT.

Keywords: *BZT–BCT lead-free ceramic, electrocaloric effect, refrigeration, doping.*

INTRODUCTION

The application of refrigeration technology covers the areas of national security, industrial and agricultural production, organic medical treatment, scientific research, and everyday life. With the rapid development of human life, the energy crisis and environmental issues are becoming more and more acute. In addition to traditional non-

[1]College of Physics, Center for Marine Observation and Communications, and National Demonstration Center for Experimental Applied Physics, Qingdao University, Qingdao, 266071, PR China.

[2]To whom correspondence should be addressed; e-mail: qdzhyc@163.com.

Published in Poroshkova Metallurgiya, Vol. 62, Nos. 3–4 (550), pp. 68–77, 2023. Original article submitted November 11, 2022.

renewable energy sources like oil and natural gas, wind and solar power generation, along with other environmentally friendly power generation methods, have been developed. Nonetheless, there are still problems like energy consumption, environmental damage, and affecting the sustainability of human beings.

At the moment, air conditioning is the most frequently used form of refrigeration, which mainly relies on traditional steam for its operation. This technology not only has low energy conversion efficiency but cannot reject using refrigerants which has a poor impact on the global environment and climate [1]. With the growing development of integrated circuits, wearable electronic devices, biotechnology, and other fields, the demand for micro-refrigeration devices is becoming more urgent. However, the traditional compressor refrigeration cannot be used for micro devices' local refrigeration due to its large volume and weight. It is necessary to find a refrigeration technology that can be miniaturized, highly efficient, energy-saving, environmentally friendly, and low-cost. Electrocaloric refrigeration has the advantages of higher refrigeration efficiency, smaller volume, environmental protection, wider working temperature range, and low cost, etc., so it is promising for refrigeration technology [2].

When an electric field is applied or removed, the isothermal entropy or adiabatic temperature change of polar crystals is called the electrocaloric effect (ECE) [3]. Kobeko and Kurtschatov first observed it in Rochelle Salt in 1930 [4]. In 1943, Hautzenlaub repeated this experiment and found that the temperature change (ΔT) of Rochelle Salt was only 0.0036 K at 1.4 kV/cm [5]. In 2006, Mischenko et al. reported in *Science* that giant electrocaloric temperature change (ΔT) of $PbZr_{0.95}Ti_{0.05}O_3$ ferroelectric thin film material was ΔT = 12 K (T = 226°C, E = = 480 kV/cm) by indirect measurement [6]. Since then, the electrocaloric effect has become a topical subject in ferroelectric materials. In 2008, Neese et al. obtained the electrocaloric temperature change (ΔT) of 12 K in PVDF ferroelectric polymer material at 209 MV/mm under room temperature [7]. Saranya et al discovered in 2009 that 0.65PMN–0.35PT thin films had an electrocaloric temperature change (ΔT) of 31 K under an electric field of 747 kV/cm and temperature of 140°C [8]. In 2014, Qian et al. established that the ΔT was 4.5 K (T = 35°C, E = = 145 kV/cm) in BZT lead-free ceramic [9]. In 2016, V. Gaurav et al. found that the giant ΔT_{max} was 52.2 K (T = = 182 K) in PZT/CFO multilayer nanostructures [10]. In 2021, Lu et al. obtained an electrocaloric temperature change (ΔT) of $(BaSr)TiO_3$ at 2.75 K (T = 21°C, E = 55 kV/cm) [11]. In 2018, S. Lu et al. established that ΔT_{max} of $0.5Ba(Zr_{0.2}Ti_{0.8})O_3$–$0.5(Ba_{0.7}Ca_{0.3})TiO_3$ was 0.464 K through the direct method [12]. In 2019, B. Nair et al. reported in *Nature* that large electrocaloric effects were observed in $PbSc_{0.5}Ta_{0.5}O_3$ over a wide temperature range [13]. In 2020, Parveen et al. found out that the enhanced electrocaloric temperature change (ΔT) of $Ba_{0.90}Sr_{0.10}Ti_{1-3x/4}Fe_xO_3$ was 1.06 K at 25 kV/cm [14]. In 2021, Suokaina et al. applied an indirect method over a broad temperature span and reported that the lead-free $Ba_{0.85}Ca_{0.15}Zr_{0.10}Ti_{0.90}O_3$(BCZT) ferroelectric ceramic relaxer was an environmentally friendly material suitable for energy storage and semiconductor electrocaloric cooling devices due to its enhanced recovered energy density (W_{rec} = 62 mJ/cm^3) and electrocaloric temperature change (ΔT) of 0.57 K [15].

Due to their excellent piezoelectricity, ferroelectricity, relaxation, low Curie temperature, and other characteristics, $BaTiO_3$-based ceramics have attracted much attention [16, 17]. But comparisons of ECE in various components of $BaTiO_3$-based ceramics show that, although there is a lot of research on ECE of $BaTiO_3$-based ceramics, it still has disadvantages on electrocaloric temperature change, operating temperature, and so on [18–23]. Doping rare earth elements has been demonstrated in previous studies to effectively introduce random fields or change the ordering degree of cations, which is conducive to improving the ferroelectric, piezoelectric, and other properties of materials [24–27]. Therefore, enhancing the local structural heterogeneity of materials is achieved by doping rare earth elements in materials. It has been proven that Sm ion is a very good rare earth element for enhancing the properties of piezoelectric materials by introducing local structural heterogeneity. For example, the piezoelectric coefficient of Sm-doped Pb-based relaxor ferroelectric ceramics and single crystals reaches as high as 1500 pC/N and 4100 pC/N, respectively, which is more than twice of the undoped samples [28–30]. Therefore, in this paper, Sm-doped 0.5BZT–0.5BCT lead-free ceramics were fabricated, and their phase structure, dielectric property, ferroelectricity, and electrocaloric effect were examined.

EXPERIMENTAL PROCEDURE

Sm-doped 0.5BZT-0.5BCT lead-free ceramic was synthesized by the conventional solid-state reaction method with $BaTiO_3$ (99.9%), $CaCO_3$ (99%), TiO_2 (99.99%), ZrO_2 (99%), Sm_2O_3 (99.9%) as raw materials. The dopant of the Sm^{3+} was 0, 1, 2, 2.5, and 3 mol.%, respectively. The preparation process is divided roughly into three parts. First, $BaTiO_3$, $CaCO_3$, TiO_2, ZrO_2, and Sm_2O_3 were mixed by using high-energy ball-milling for 1 h and calcined at 1,250°C for 3 h to form BZT–BCT powders. Then, a green body 13 mm in diameter was formed by dry pressing. Lastly, oxygen atmosphere sintering and hot sintering were used to synthesize the BZT–BCT lead-free ceramic.

The phase structure of Sm-doped 0.5BZT–0.5BCT ceramic was characterized by X-ray diffraction (XRD, Smart Lab, Rigaku, Japan). Scanning electron microscopy (SEM, JSM-6390LV, JEOL, Japan) was used to observe the microstructure of the fracture surface. A precision impedance analyzer (4294 A) from Agilent (USA) was used to measure the frequency dependence of dielectric permittivity. The ferroelectric hysteresis *P-E* loops were measured by a ferroelectric test system (RT Premier II, Radiant, USA). The ceramics were measured directly under vacuum adiabatic conditions using a homemade electrocaloric instrument. The details can be viewed in [31].

RESULTS AND DISCUSSION

High performance requires ceramics that have a high pure perovskite-structure phase. The XRD pattern of 0.5BZT–0.5BCT lead-free ceramics with different Sm doping contents is shown in Fig. 1*a*.

It is evident that the ceramics with different Sm doping content are all typical perovskite-structure phases without any other secondary phase present. Under the same measurement conditions, it is commonly agreed upon that the higher the intensity of the diffraction peak, the lower the full-width half maximum (FWHM), i.e., the narrower the peak, the better the crystalline of the crystal. According to Fig. 1*a*, all diffraction peaks of 3 mol.% Sm-doped ceramics are more intense and sharper than other components under the same measurement conditions. The increase of Sm doping amount under the same sintering conditions results in a better crystallinity and sintering degree of ceramics [32, 33]. No peak splitting was observed in the enlarged (200) peak in Fig. 1*b*, and the slightly asymmetrical diffraction peak demonstrates that those compositions are located at the morphotropic phase boundary (MPB) [34]. The diffraction peaks (200) gradually move to a small angle with the increase in Sm doping content.

From Fig. 2, the fracture surface of 0.5BZT–0.5BCT lead-free ceramics with different Sm doping contents is shown in the SEM images in Fig. 2. Transgranular fracture is present in all the samples and there are no clear grain boundaries. The region where the energy expenditure is the lowest for a ceramic when subjected to external stress tends to fracture, i.e., where the bonding between atoms or ions (chemical bond) is weakest. The transgranular fracture indicates that there is a greater lattice binding at the grain boundaries than inside the grain. Furthermore, there are few pores that have a negative impact on the breakdown field strength of all doped ceramics, which can be used to adjust the electrocaloric temperature (ΔT).

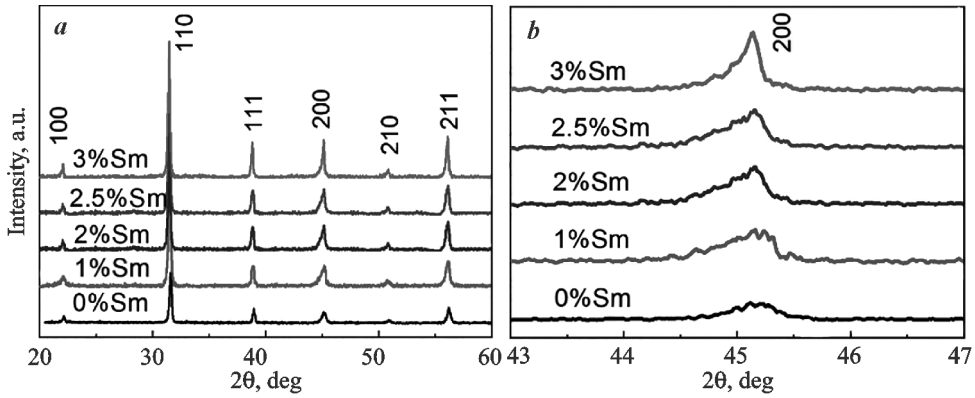

Fig. 1. XRD patterns (*a*) and enlarged (200) diffraction peaks (*b*) of Sm-doped 0.5BZT–0.5BCT ceramics

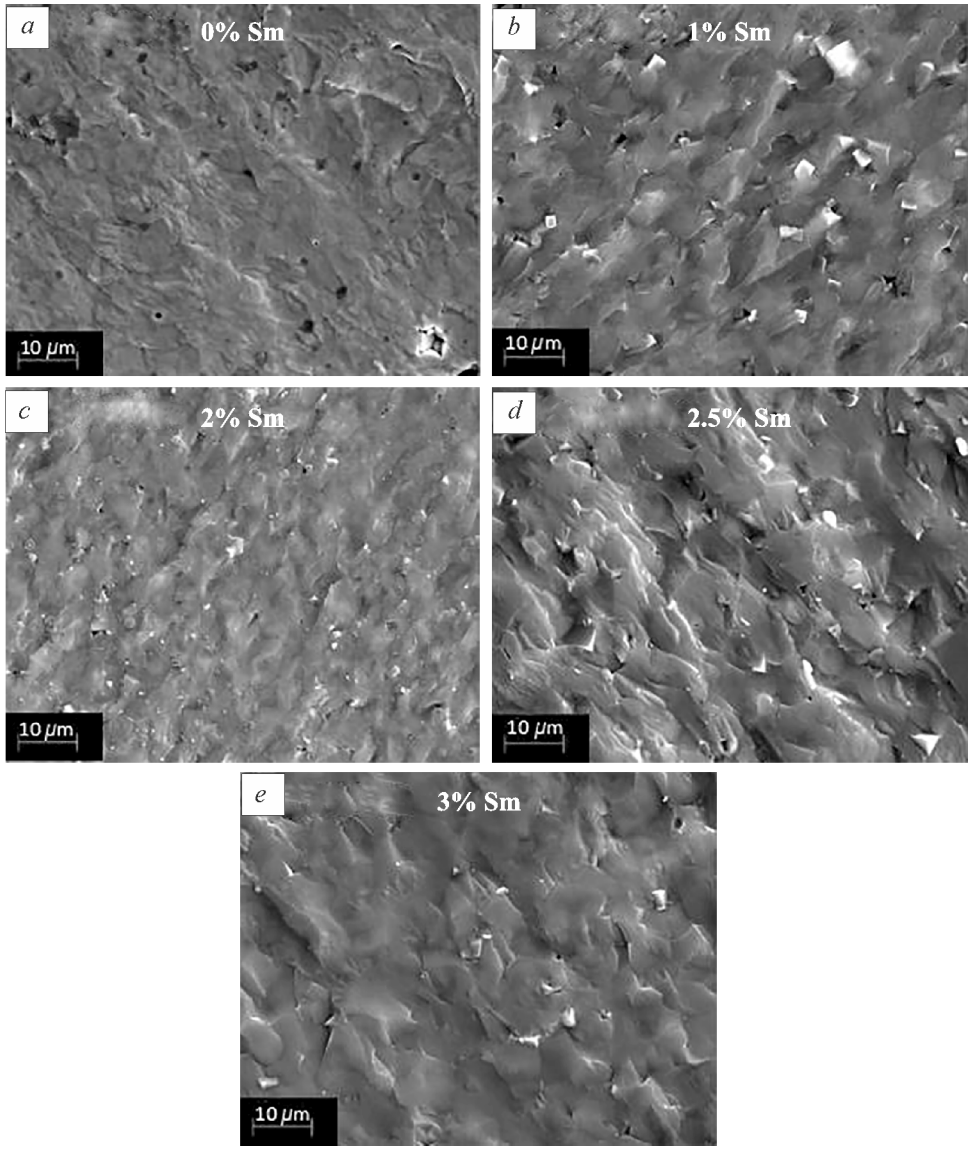

Fig. 2. SEM images of Sm-doped 0.5BZT–0.5BCT lead-free ceramics

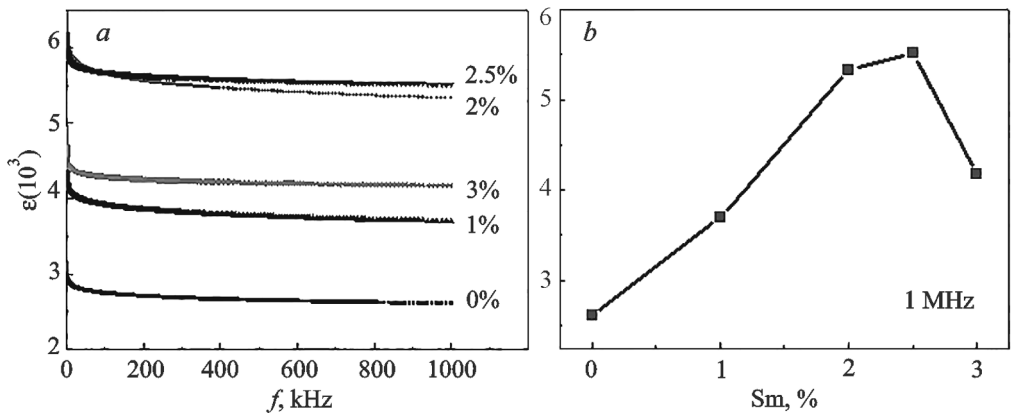

Fig. 3. Frequency dependence of dielectric permittivity (*a*) and the changing trend of dielectric permittivity (*b*) with Sm doping amount of 0.5BZT–0.5BCT ceramics

The frequency dependence of dielectric permittivity of 50BZT–50BCT lead-free ceramics doped with different contents of Sm is shown in Fig. 3. As it can be seen from Fig. 3*a*, the dielectric permittivity of the ceramics decreases slightly with the increase of frequency. The reason for this is that the dielectric permittivity is primarily dependent on the orientation polarization of the inherent dipole moment. As frequency increases, the orientation polarization of the inherent dipole moment cannot keep up with the rapid change of the electric field. Thus, the inherent dipole moment orientation's polarization contribution decreases, which indicates a decline in dielectric permittivity [35]. By comparing the dielectric permittivity of the ceramics with different doping amounts of Sm at 1 MHz, the dielectric permittivity first increases and then decreases with the increase of Sm doping contents (Fig. 3*b*). It is worth noting that the maximum dielectric permittivity is 5,518 when the doping content of Sm is 2.5 mol.%. The dielectric properties of relaxor ferroelectrics can be improved by the addition of an appropriate dopant of rare earth elements [28].

Since the electrocaloric effect is related to the polarization (*P*), the strength of ferroelectricity is a very crucial factor in the ECE [36]. Ferroelectric hysteresis (*P–E*) loops of the 0.5BZT–0.5BCT lead-free ceramics with different doping content of Sm are shown in Fig. 4. With the increase of Sm^{3+} doping content, the *P–E* loops become slimmer and more inclined, indicating that the relaxation of 0.5BZT–0.5BCT ceramics is enhanced [37]. It is well-known that normal ferroelectrics are made up of a large number of domains with long-range ordering states,

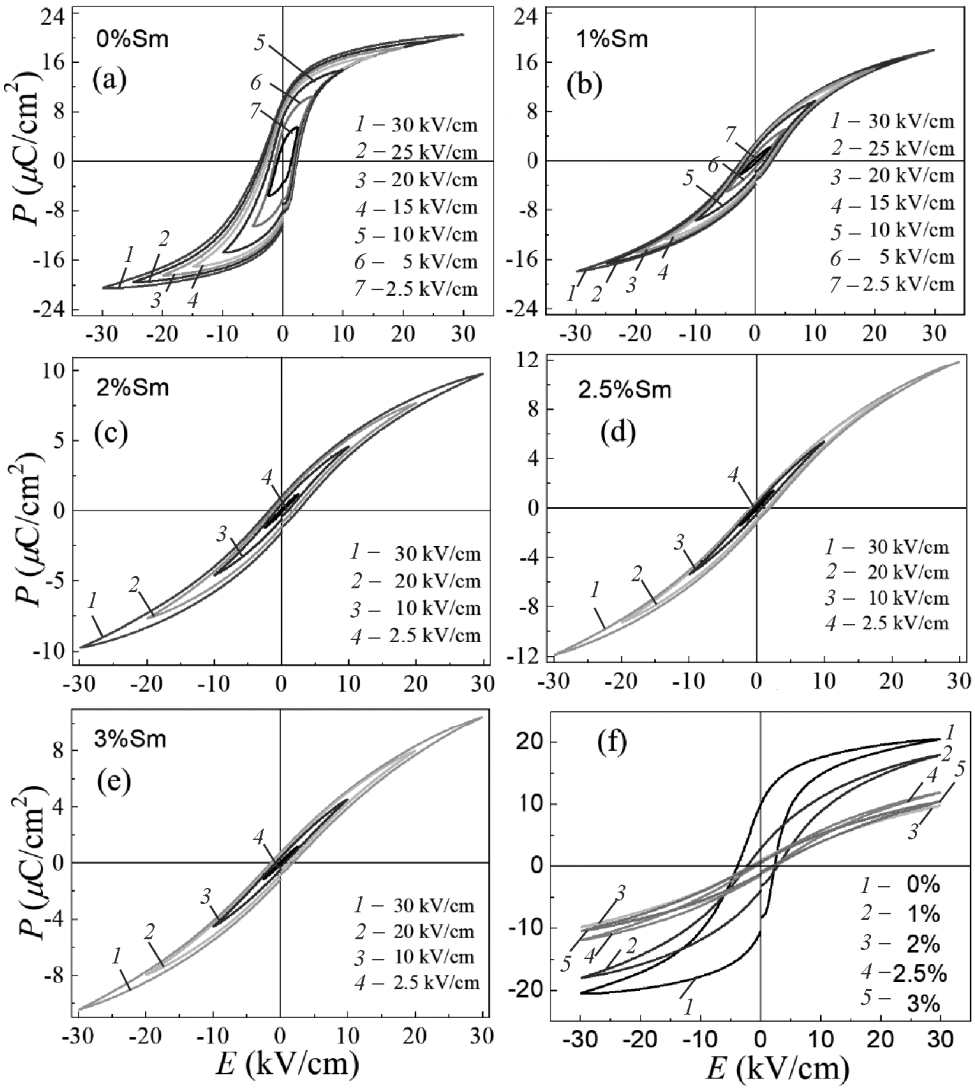

Fig. 4. *P–E* loops of Sm-doped 0.5BZT–0.5BCT lead-free ceramics

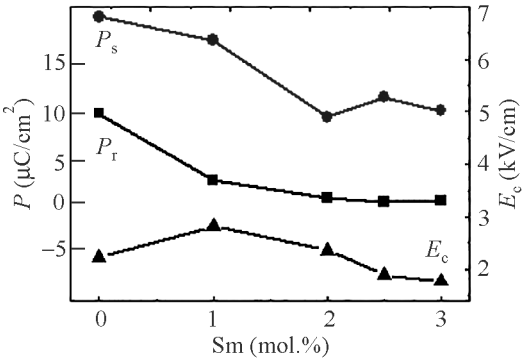

Fig. 5. E_c, P_s, and P_r as a function of Sm doping content in 0.5BZT–0.5BCT lead-free ceramics

while relaxor ferroelectrics have polar nanodomains. That is to say, with the increase of Sm doping, more polar nanoregions (PNRs) are formed in BZT–BCT lead-free ceramics doped by Sm [28].

Figure 5 shows the variation of the polarization (P) and coercive field (E_c) of 0.5BZT–0.5BCT lead-free ceramics with different Sm doping content at 30 kV/cm extracted from Fig. 4. As can be seen from Fig. 5, P value of the ceramics decrease gradually. That is because when Sm^{3+} replaces the Ba^{2+} at the A site. By changing the long-range ordering degree of the oxygen octahedron, the stability, and ferroelectricity of materials will be reduced. In addition, the coercive field (E_c) increases first and then decreases with the increase of Sm doping content.

The electrocaloric temperature change of 0.5BZT–0.5BCT lead-free ceramics with different Sm doping contents measured through the direct method is shown in Fig. 6. The electrocaloric temperature change (ΔT_D) of ceramics with different doping contents of Sm is shown in Fig. 6*a* under an electric field of 4 kV/mm at room temperature. Figure 6*a* shows that the electrocaloric temperature change (ΔT_D) increases first and then decreases with an increase in Sm doping. Among them, the ΔT_{Dmax} is 0.109 K when the doping content of Sm is 2 mol.%. The applied electric field and the measurement temperature will affect the ΔT_D values. Compared with the previous research by Lu et al., they obtained the ΔT_{max} of 0.464 K in undoped 0.5BZT–0.5BCT at the electric field of 6 kV/mm and the temperature of 100°C [12]. A larger electric field and higher temperature close to Curie temperature will lead to higher ΔT_D values. Therefore, the ΔT_D values can be further improved by adjusting measurement conditions. Furthermore, the electrocaloric effect curves measured directly are deformed to a certain extent. That indicates that the leakage current of materials causes a large joule heating under the electric field of 4 kV/mm [38–41].

Figure 6*b* shows the electrocaloric temperature change (ΔT_D) of different Sm-doped ceramics under different electric fields. As can be seen from the figure, as the electric field increases, the electrocaloric temperature change of materials gradually increases, and the ΔT_{max} is achieved when the dopant of Sm^{3+} is 2 mol.%.

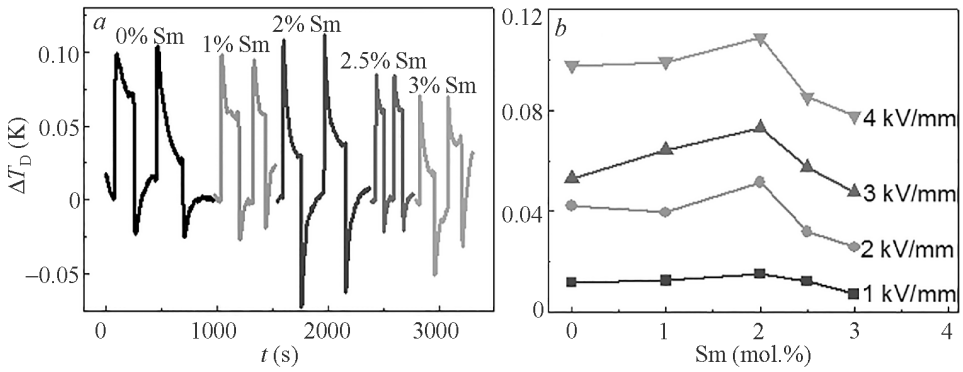

Fig. 6. Curves of electrocaloric temperature change measured by the direct method (*a*) and ΔT_D as a function of Sm doping content of 0.5BZT–0.5BCT ceramics (*b*)

CONCLUSIONS

The effect of Sm doping content on the structure and properties of 0.5BZT–0.5BCT lead-free ferroelectric ceramics was systematically studied. XRD patterns indicate that all of the Sm-doped 0.5BZT–0.5BCT ceramics are pure perovskite phase. With the increase of Sm doping content, the ferroelectric hysteresis (*P–E*) loops of 0.5BZT–0.5BCT ceramics become slimmer and more inclined, indicating the relaxation of ceramics is gradually enhanced. The increase of Sm doping content results in a first decrease in the dielectric permittivity, followed by an increase in the dielectric permittivity. The maximum dielectric permittivity at 1 MHz reaches 5,518 when the Sm dopant is 2.5 mol.%. The electrocaloric temperature change (ΔT) increases first and then decreases with the increase of Sm content. The maximum electrocaloric temperature change (ΔT_{max}) is 0.109 K (E = 4 kV/mm, room temperature) at the Sm doping content of 2 mol.%. It indicates that an appropriate Sm doper is beneficial in improving the dielectric, ferroelectric, and electrocaloric properties of 0.5BZT–0.5BCT lead-free ceramics.

AUTHORS CONTRIBUTIONS

Fengji Zheng and Shijuan Lu share equal contributions to this work.

ACKNOWLEDGMENTS

This work is financially supported by the National Natural Science Foundation of China (52272116), the Natural Science Foundation of Shandong Province (ZR2021ME096), and the Youth Innovation Team Project of Shandong Provincial Education Department (2019KJJ012).

DECLARATIONS

There are no conflicts of interest between the authors.

REFERENCES

1. B. Peng, H. Fan, and Q. Zhang, "A Giant electrocaloric effect in nanoscale antiferroelectric and ferroelectric phases coexisting in a relaxor $Pb_{0.8}Ba_{0.2}ZrO_3$ thin film at room temperature," *Adv. Funct. Mater.*, **23**, 2987–2992 (2013).
2. X. Moya, S. Kar-Narayan, and N.D. Mathur, "Caloric materials near ferroic phase transitions," *Nat. Mater.*, **13**, No. 5, 439–450 (2014).
3. Annual Review of Materials Research, *Mater. Sci.*, **41**, 229–240 (2011).
4. P. Kobeko and J. Kurtschatov, "Dielektrische Eigenschaften der Seignettesalzkristalle," *Zeitschrift für Physik,* **66**, 192–205 (1930).
5. G.G. Wiseman and J.K. Kuebler, "Electrocaloric effect in ferroelectric rochelle salt," *Phys. Rev.*, **131**, 2023–2027 (1963).
6. A.S. Mischenko, Q. Zhang, J.F. Scott, R.W. Whatmore, and N.D. Mathur, "Giant electrocaloric effect in thin-film $PbZr(0.95)Ti(0.05)O_3$," *Science,* **37**, 1270–1271 (2006).
7. B. Neese, B.J. Chu, S.G. Lu, Y. Wang, E. Furman, and Q.M. Zhang, "Large electrocaloric effect in ferroelectric polymers near room temperature," *Science*, **321**, 821–823 (2008).
8. D. Saranya, A.R. Chaudhuri, J. Parui, and S.B. Krupanidhi, "Electrocaloric effect of PMN-PT thin films near morphotropic phase boundary," *Bull. Mater. Sci.*, **32**, 259–262 (2009).
9. X.S. Qian, H.J. Ye, Y.T. Zhang, H. Gu, X. Li, C.A. Randall, and Q.M. Zhang, "Giant electrocaloric response over a broad temperature range in modified $BaTiO_3$ ceramics," *Adv. Funct. Mater.*, **24**. 1336 (2014).
10. G. Vats, A. Kumar, N. Ortega, C.R. Bowen, and R.S. Katiyar, "Giant pyroelectric energy harvesting and a negative electrocaloric effect in multilayered nanostructures," *Energ. Environ. Sci.*, **9**, 1335–1345 (2016).
11. X. Niu, X.B. Jian, X.Y. Chen, H.X. Li, W. Liang, Y.B. Yao, T. Tao, B. Liang, and S.G. Lu, "Enhanced electrocaloric effect at room temperature in Mn^{2+} doped lead-free $(BaSr)TiO_3$ ceramics via a direct measurement," *J. Adv. Ceram.*, **10**, 482–492 (2021).

12. S.J. Lu, G.R. Chen, Y.C. Zhang, Z.M. Zhao, F. Li, Z.L. Lv, Z.M. Ma, D.D. Wang, C.J. Lu, and S.D. Li, "Electrocaloric effect in lead-free $0.5Ba(Zr_{0.2}Ti_{0.8})O_3 0.5(Ba_{0.7}Ca_{0.3})TiO_3$ ceramic measured by direct and indirect methods," *Ceram. Int*., **44**, No. 17, 21950–21955 (2018).
13. B. Nair, T. Usui, S. Crossley, S. Kurdi, G.G. Guzmán-Verri, X. Moya, S. Hirose, and N.D. Mathur, "Large electrocaloric effects in oxide multilayer capacitors over a wide temperature range," *Nature*, **575** (7783), 468–472 (2019).
14. P. Kumar and C. Prakash, "Enhanced electrocaloric effect in lead free $Ba_{0.90}Sr_{0.10}Ti_{1-3x/4}Fe_xO_3$ ceramics," *J. Alloy. Compd*., **839**, 155461 (2020).
15. S. Merselmiz, Z. Hanani, D. Mezzane, A.G. Razumnaya, and Z. Kutnjak, "Thermal-stability of the enhanced piezoelectric, energy storage and electrocaloric properties of a lead-free BCZT ceramic," *Rsc. Adv*., **11** (16), 9459–9468 (2021).
16. M. Acosta, N. Khakpash, T. Someya, N. Novak, W. Jo, H. Nagata, G.A. Rossetti Jr, and J. Roedel, "Origin of the large piezoelectric activity in $(1-x)Ba(Zr_{0.2}Ti_{0.8})O_3–x(Ba_{0.7}Ca_{0.3})TiO_3$," *Ceramics, Phys. Rev. B*, **91**, No. 10, 104108 (2015).
17. X. Niu, X.D. Jian, W.P. Gong, W. Liang, X.T. Gong, G.Z. Zhang, S.L. Jiang, K. Yu, X.B. Zhao, Y.B. Yao, T. Tao, B. Liang, and S.G Lu, "Field-driven merging of polarizations and enhanced electrocaloric effect in $BaTiO_3$-based lead-free ceramics," *J. Adv. Ceram*., **11**, No. 11, 1777–1788 (2022).
18. J. Wang, T. Yang, S. Chen, L. Gang, Q. Zhang, and Y. Xi, "Nonadiabatic direct measurement electrocaloric effect in lead-free $Ba,Ca(Zr,Ti)O_3$ ceramics," *J. Alloy. Compd*., **550**, 561–563 (2013).
19. B. Yang, H. Xi, and L. Qiao, "Optimized electrocaloric refrigeration capacity in lead-free $(1–x)BaZr_{0.2}Ti_{0.8}O_3–xBa_{0.7}Ca_{0.3}TiO_3$ ceramics," *Appl. Phys. Lett*., **102**, No. 25, 1270 (2013).
20. M. Sanlialp, V.V. Shvartsman, M. Acosta, B. Dkhil, and D.C. Lupascu, "Strong electrocaloric effect in lead-free $0.65Ba(Zr_{0.2}Ti_{0.8})O_3–0.35(Ba_{0.7}Ca_{0.3})TiO_3$ ceramics obtained by direct measurements," *Appl. Phys. Lett*., **106**, 062901 (2015).
21. M. Sanlialp, V.V. Shvartsman, M. Acosta, and D.C. Lupascu, "Electrocaloric effect in $Ba(Zr,Ti)O_3$–$(Ba,Ca)TiO_3$ ceramics measured directly," *J. Am. Ceram. Soc*., **99**, No. 12, 4022–4030 (2016).
22. Y. Zhou, Q. Lin, W. Liu, and D. Wang, "Compositional dependence of electrocaloric effect in lead-free $(1–x)Ba(Zr_{0.2}Ti_{0.8})O_3–x(Ba_{0.7}Ca_{0.3})TiO_3$ ceramics," *Rsc. Adv*., **6**, No. 17, 14084–14089 (2016).
23. X.D. Jian, B. Lu, D.D. Li, Y.B. Yao, T. Tao, B. Liang, J.H. Guo, Y.J. Zeng, J.L. Chen, and S.G. Lu, "Direct measurement of large electrocaloric effect in $Ba(Zr_xTi_{1-x})O_3$ ceramics," *ACS Appl. Mater. Inter*., **10**, No. 5, 4801–4807 (2018).
24. W. Kleemann, "Relaxor ferroelectrics: Cluster glass ground state via random fields and random bonds," *Phys. Status. Solidi. B*, **251**, No. 10, 1993–2002 (2014).
25. M. Zhang, W.L. Wang, G.T. Xia, L.C. Wang, and K. Wang, "Self-powered electronic skin for remote human-machine synchronization," *ACS Appl. Electron. Mater*., **5**, No. 1, 498–508 (2023).
26. F. Li, S. Zhang, T. Yang, Z. Xu, N. Zhang, G. Liu, J. Wang, J. Wang, Z. Cheng, Z.G. Ye, J. Luo, T.R. Shrout, and L.Q. Chen, "The origin of ultrahigh piezoelectricity in relaxor-ferroelectric solid solution crystals," *Nat. Commun.*, **7**, 13807 (2016).
27. H. Takenaka, I. Grinberg, S. Liu, and A.M. Rappe, "Slush-like polar structures in single-crystal relaxors," *Nature*, **546**, 391–395 (2017).
28. F. Li, D. Lin, Z.B. Chen, Z.X. Cheng, J.L. Wang, C.C. Li, Z. Xu, Q.W. Huang, X.Z. Liao, L.Q. Chen, T.R. Shrout, and S.J. Zhang, "Ultrahigh piezoelectricity in ferroelectric ceramics by design," *Nat. Mater*., **17**, No. 4, 349–354 (2018).
29. F. Li, M.J. Cabral, B. Xu, Z. Cheng, E.C. Dickey, J.M. Lebeau, J. Wang, J. Luo, S. Taylor, W. Hackenberger, L. Bellaiche, Z. Xu, L. Chen, T.R. Shrout, and S. Zhang, "Giant piezoelectricity of Sm-doped $Pb(Mg_{1/3}Nb_{2/3})O_3–PbTiO_3$ single crystals," *Science*, **364**, 264–268 (2019).

30. F.J. Zheng, X. Tian, Z. Fang, J.F. Lin, Y. Lu, W. Gao, R. Xin, D.S. Fu, Y. Qi, Z.Z. Ma, W.N. Ye, Y.L. Qin, X.X. Wang, and Y.C. Zhang, "Sm-doped PIN-PMN-PT transparent ceramics with high Curie temperature, good piezoelectricity, and excellent electro-optical properties," *ACS Appl. Mater. Inter*.," **15**, No. 5, 7053–7062 (2023).
31. G. Chen, Y. Zhang, X.M. Chu, G. Zhao, F. Li, J. Zhai, Q. Ren, B. Li, and S. Li, "Large electrocaloric effect in La-doped $0.88Pb(Mg_{1/3}Nb_{2/3})O_3$–$0.12PbTiO_3$ relaxor ferroelectric ceramics," *J. Alloy. Compd*., **727**, 785–791 (2017).
32. S. Guo, B. Luo, H. Xing, J. Wang, H.M. Zeeshan, K. Jin, and C. Chen, "Ferroelectric, dielectric, and impedance properties of Sm-modified $Ba(Zr_{0.2}Ti_{0.8})O_3$–$x(Ba_{0.7}Ca_{0.3})TiO_3$ ceramics," *Ceram. Int*., **46**, No. 6, 7198–7203 (2020).
33. A.R. Jayakrishnan, K.V. Alex, A. Thomas, J.P.B. Silva, K. Kamakshi, N. Dabra, K.C. Sekhar, J.A. Moreira, and M.J.M. Gomes, "Composition-dependent xBa$(Zr_{0.2}Ti_{0.8})O_3$–$(1–x)(Ba_{0.7}Ca_{0.3})TiO_3$ bulk ceramics for high energy storage applications," *Ceram. Int*., **45**, No. 5, 5808–5818 (2018).
34. C. Li, B. Xu, D. Lin, S. Zhang, F. Li, L. Bellaiche, and T.R. Shrout, "Atomic-scale origin of ultrahigh piezoelectricity in samarium-doped PMN–PT ceramics," *Phys. Rev. B*, **101**, 140102 (2020).
35. M. Rao and R. Pandit, "Magnetic and thermal hysteresis in the O(N)-symmetric $(\Phi^2)^3$ model," *Phys. Rev. B*, **43**, No. 4, 3373–3386 (1991).
36. Lang B. Sidney, "Cryogenic refrigeration utilizing the electrocaloric effect in pyroelectric lithium sulfate monohydrate," *Ferroelectrics,*" **11**, No. 1, 519–523 (1976).
37. D. Fu, H. Taniguchi, M. Itoh, S.Y. Koshihara, N. Yamamoto, and S. Mori, "Relaxor $Pb(Mg_{1/3}Nb_{2/3})O_3$: A ferroelectric with multiple inhomogeneities," *Phys. Rev. Lett.*, **103**, 207601 (2009).
38. M. Quintero, L. Ghivelder, F. Gomez-Marlasca, and F. Parisi, "Decoupling electrocaloric effect from Joule heating in a solid state cooling device," *Appl. Phys. Lett.*, **99**, 232908 (2011).
39. M. Quintero, P. Gaztanaga, and I. Irurzun, "Intrinsic leakage and adsorption currents associated with the electrocaloric effect in multilayer capacitors," *Appl. Phys. Lett*., 107, No. 15, 229–240 (2015).
40. Y. Qin, J. Yang, P. Xiong, W. Huang, J. Song, L. Yin, P. Tong, X. Zhu, and Y. Sun, "The effects of quenching on electrical properties, and leakage behaviors of $0.67BiFeO_3$–$0.33BaTiO_3$ solid solutions," *J. Mater. Sci. Mater. Electron*., **29**, No. 9, 7311–7317 (2018).
41. S.J. Lu, J.H. Li, M.Q. Cheng, Q.C. Li, F. Li, Z.L. Lv, Y.C. Zhang, C.J. Lu, and S.D. Li, "Joule heating – A significant factor in the electrocaloric effect," *Ceram. Int*., **45**, No. 14, 16992–16998 (2019).